



Synthesis, Characterization, Morphology and Mechanical properties of SBR-nanocomposites Derived from Nano Antimony Oxide

Rani V Mankar, Wasudeo B Gurnule*

Post Graduate Department of Chemistry, Kamla Nehru Mahavidyalaya, Nagpur, 440024, India

ABSTRACT

A novel rubber-nanocomposite has been synthesized through the emulsion polymerization of styrene-butadiene rubber and nano antimony oxide using accelerators and antioxidant. Sulphur was used as vulcanizing agent. The synthesized SBR-nano antimony oxide was characterized by elemental analysis, FTIR, scanning electron microscopy, transmission electron microscopy and mechanical testing. On basis of the FTIR, the structure of the SBR-nano antimony oxide was proposed. The physico-chemical parameters have been evaluated for the SBR-nano antimony oxide. The aggregation nature of the synthesized rubber-nano composite was established by scanning electron microscopy (SEM). The effects of nano particles in polymer matrices have been evaluated for the SBR-nano antimony from TEM analysis. Mechanical behavior of the composites are found to improve consistently as nano- antimony oxide content in the composites increases owing to increased rubber- filler interaction. Tensile strength studies are found to be useful to assess the improvement of the mechanical properties of matrix.

Keywords: Synthesis, Characterization, Morphology, Nano antimony oxide, Mechanical properties.

INTRODUCTION

The mechanical reinforcement of polymer matrices by nano particles is a fundamental problem with far reaching applications, e.g., for car tires [1]. Since the days of pioneering works of Harkins [2] and Smith and Ewart [3], many advances were made in the understanding of kinetics of emulsion polymerization, mainly in the area of interfacial processes like radical entry and exit into and out of the polymer particles [4,5]. From a conceptual point of view, it is generally recognized that the filler structure has a strong impact on the mechanical properties [6,7], accompanied by the effect of chain structure evolving in the hard filler environment [8-11], and the filler-chain interactions [12-17]. However, some important aspects of the process, like polymer particles nucleation and coagulation, still lack proper description and explanation [18]. All these contributions are related to the filler structure, and it is thus important to be able to characterize it in detail. The general framework for the modeling of emulsion copolymerization reactors as well as the synoptical overview of existing studies on this topic was provided by Saldivar et al. [19]. Unfortunately, two typical situations are usually encountered: either the system is a model system of individually dispersed nano particles [20], which is easier to understand but is further away from applications, or the system is made by mixing of powders of aggregated nano particles, together with many additives, and analysis becomes difficult. Conzatti et al have investigated the morphology of the same silica in SBR by TEM with automated image analysis, and dynamic mechanical analysis (DMA), varying the surface modification [21]. Kanetakis et al. [22] used the residence time distribution (RTD) for modeling the polymer particle size distribution for the SBR production in the cascade of six to nine continuous stirred tank reactors. Ramier et al have studied the silica structure in SBR by transmission electron microscopy (TEM) and small-angle X-ray scattering (SAXS), without further analysis of the SAXS-data as they focused on the rheology [23].

In this work, we prepared SBR-nano composites copolymer with the use of nano antimony oxide as filler by emulsion polymerization method. The effect of nano antimony oxide on the elemental, spectral, morphology and mechanical properties has been studied. Elemental analysis, Fourier Transform Infrared (FTIR), morphology and mechanical properties are carried out for all five composites.

MATERIALS AND METHODS

Materials

Nano composites were purchased from centre scientific company Nagpur, India. Tetramethyl thiuram disulfide, 2, 2'- dithiobis, stearic acid and N, N'- Diphenyl P- phenylene diamine were purchased from centre scientific company Nagpur, India. Zinc oxide and sulphur (from Post Graduate Departement of chemistry Kamla Nehru Mahavidyalaya, Nagpur, India). Styrene butadiene rubber latex purchased from shree Radha Polymer company, Nagpur, India.

Preparation of SBR- nano composite

First, nano antimony oxide was dispersed in toluene with vigorous stirring and nano antimony oxide suspension was obtained at room temperature. Then SBR latex was added into the nano antimony oxide suspension and stirred upto uniform mixing of SBR into the nano antimony oxide. The mixture was coagulated at room temperature. Then washed with water several times and then dried at 70°C for 12 h. Then SBR-nano compound was formed.

Compounding of rubber

SBR- nano compound was mixed with various ingredients shown in the Table 1. The SBR- nano compound then was vulcanized at 150°C. The mixture of SBR- nano compound were directly used on two- roll mill and mixing for 15 min, then adding all necessary ingredients which are listed in Table 1 and mixing for 10 min. After that the resultant compound were vulcanized at 150°C.

Table 1: Formulation of rubber compound

Ingredients	Phr				
	1	2	3	4	5
SBR	100	100	100	100	100
Nano antimony oxide	0	2	6	10	12
Stearic acid	2	2	2	2	2
Zinc oxide	5	5	5	5	5
2, 2'- dithiobis	0.5	0.5	0.5	0.5	0.5
Tetramethyl thiuram disulfide (TMTD)	0.2	0.2	0.2	0.2	0.2
N, N'- Diphenyl P- phenylene diamine	1	1	1	1	1
Sulphur	2	2	2	2	2

Characterizations*Fourier-transform infrared spectroscopy (FTIR)*

FTIR spectra of SBR- nano composites were determined by using a shimadzu IR- Affinity spectrophotometer (from Dept. of Chemistry Kamla Nehru Mahavidyalaya, Nagpur, India).

Scanning electron microscopy (SEM)

Surface morphology of the nano composites was investigated by using Scanning electron microscope JEOL (JSM- 6390, SAIF, cochin) at an acceleration voltage of 3 KV. Due to the very narrow electron beam, SEM micrographs have a large depth of field yielding a characteristic three-dimensional appearance useful for understanding the surface structure of samples.

Transmission electron microscopy (TEM)

Morphology of SBR nano composites was directly observed by Transmission electron microscope (Model JEM 2100) at an accelerating voltage of 200 kV. Ultra-thin film of nano composite (less than 100 nm) obtained by ultra-microtome cutting under cryogenic conditions was used for the morphological studies (from IIT Bombay).

Mechanical tests

To examine tensile strength, elongation at break and tear resistance properties use a tensile Monsanto T10 Tensometer according to the ASTM D412. It consisting of two jaws, one fixed and the other moving quickly 500 mm/min (from Mumbai University).

Abrasion resistance

Testing is done by device type (wallace test equipment, HZ 50) as ASTM D2228. The device works with 250 W, where the sample is placed touching the lever, the lever spin 500 cycle for 5 min (from Mumbai University) and then calculated the difference in weight before and after the test.

Swelling study

The crosslinking density of all the vulcanized samples was determined by the equilibrium swelling method using toluene as solvent. The cured samples of known weight were allowed to swell for 7 days in fresh toluene at room temperature. After each 24 hour solvent were changed with fresh toluene. After 7 days, samples were taken out and adhered liquid was rapidly removed by blotting with tissue paper and weighed immediately. It was vacuum dried at 80°C till a constant weight was obtained. Crosslinking density V_e , defined by the number of elastically active chains per unit volume was determined by Flory–Rehner eqn 1 [24].

$$V_e = -[\ln(1 - V_r) + V_r + X_1 V_r^2] / [V_1 (V_r^{1/3} - V_r/2)] \quad (1)$$

where, V_e is the network chain density, V_1 is the molar volume of the toluene ($106.3 \text{ cm}^3 \text{ mol}^{-1}$), V_r is the volume fraction of rubber in swollen network and X_1 is the Flory–Huggins rubber– solvent interaction parameter.

RESULTS AND DISCUSSION**Elemental analysis**

All the five rubber nano composites were analyzed at Sophisticated Analytical Instrumentation Facility, STIC, Cochin University, Cochin for C,

H, N and S. The empirical formula for all the five SBR, SBR- Antimony oxide (2 phr), SBR-Antimony oxide (6 phr), SBR- Antimony oxide (10 phr) and SBR- Antimony oxide (12 phr) were determined on the basis of C, H, N and S by messenger method. The observed results are found to be in good agreement with the calculated values. From the empirical formula, the empirical weight of a single repeating unit was calculated. Analytical data for all the five SBR- Antimony oxide nano composites are presented in Table 2.

Table 2: Elemental analysis data of Styrene-Butadiene rubber-antimony oxide composites

Rubber samples	% of C observed (Cal.)	% of H observed (Cal.)	% of N observed (Cal.)	% of O observed (Cal.)	% of S observed (Cal.)	Empirical Formula	Empirical Weight
SBR	83.44	8.11	2.56	5.85	2.34	$C_{38}H_{44}N_1O_2S$	546.993
	(81.44)	(8.05)	(2.31)	(5.08)	(1.39)		
SBR-Antimony oxide (2 phr)	79.12	8.82	2.36	5.4	3.41	$C_{39}H_{46}N_1O_2S_1$	592.862
	(79.87)	(8.78)	(2.21)	(5.38)	(3.7)		
SBR-Antimony oxide (6 phr)	79.9	9.69	2.3	5.24	5.27	$C_{40}H_{50}N_1O_2S_1$	608.955
	(81.2)	(8.99)	(2.1)	(5.01)	(5.02)		
SBR- Antimony oxide (10 phr)	79.45	8.65	2.23	5.04	5.05	$C_{42}H_{52}N_1O_2S_1$	634.943
	(81.2)	(8.89)	(2.3)	(4.6)	(5.05)		
SBR- Antimony oxide (12 phr)	78.89	8.87	2.2	6.26	5.58	$C_{42}H_{52}N_1O_4S_1$	666.941
	(79.67)	(9.12)	(2.12)	(5.2)	(5.02)		

FTIR spectroscopy

Figure 1 shows FTIR (Fourier- transform infrared spectroscopy) spectra of different loadings levels of antimony oxide. In all these spectra, the broad peak at $3,400\text{ cm}^{-1}$ is assigned to stretching vibration of $-\text{OH}$ group stretching vibrations along with adsorbed water. The peaks at 950 cm^{-1} and 860 cm^{-1} are due to C-H bending of aromatic ring in antimony oxide. The peak at 1100 cm^{-1} and 470 cm^{-1} are due to antisymmetric and symmetric stretching. The presence of two sharp peaks at $2,930\text{ cm}^{-1}$ and $2,840\text{ cm}^{-1}$ and one peak around $1,450\text{ cm}^{-1}$ for all the spectra of SBR-filler in addition of the absorption bands corresponding to the vibration of specific functional group. These small peaks of around $2,930\text{ cm}^{-1}$ and $2,840\text{ cm}^{-1}$ are characteristic bands of symmetric and antisymmetric stretching vibrations of $-\text{CH}_2$ group respectively; $1,450\text{ cm}^{-1}$ corresponding to bending vibrations of $-\text{CH}_2$ group. All these peaks are observed in spectra of SBR-nano composites in Figure 1. This is also supported by the presence of band at 1080 cm^{-1} which is characteristic band of alkene group. The peak at 1750 cm^{-1} of antimony oxide before and after CO activation which indicates the presence of $\text{C}=\text{O}$ functional groups characterized by aldehydes, ketones, carboxylic acids and esters. The presence of band at 2550 cm^{-1} , which is characteristic band of $\text{C}=\text{C}$ aromatic group. In the case of antimony oxide, the filler-polymer interaction is mainly of physical nature.

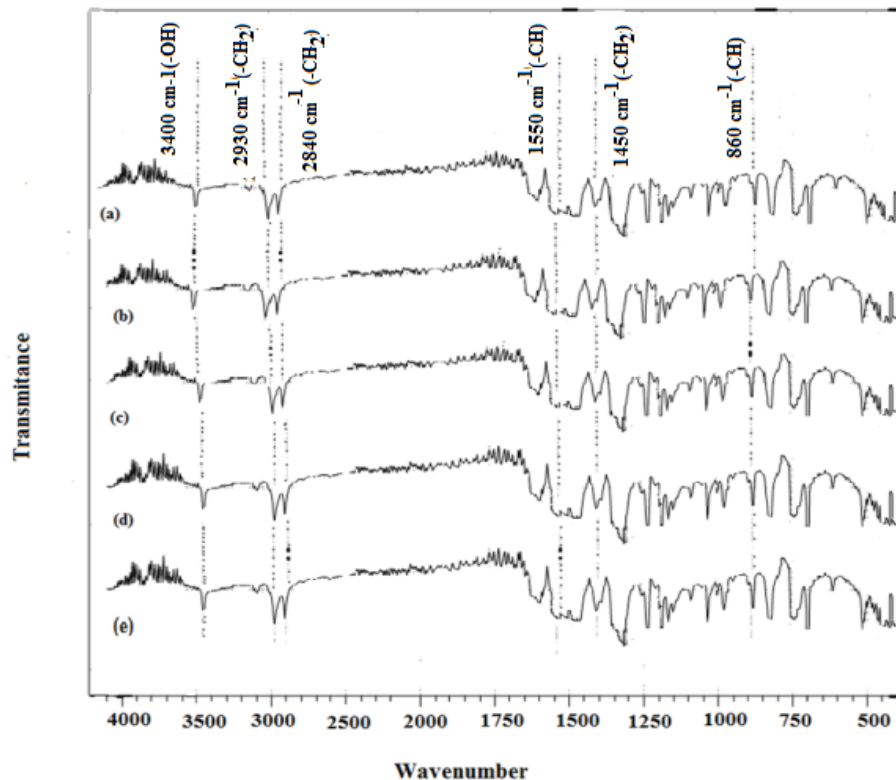


Figure 1: FTIR (Fourier- transform infrared spectroscopy) spectra of SBR- nano composite (a) unfilled composites (b) 2 phr antimony oxide in SBR (c) 6 phr antimony oxide in SBR (d) 10 phr antimony oxide in SBR (e) 12 phr antimony oxide in SBR

Scanning electron microscopy

According to Figure 2, a satisfactory volumetric homogeneity can be observed for all samples investigated indicating that set of parameters assigned to the preparation method, system and vulcanization parameters used were appropriate. SEM micrographs in Figures 2a-2d show the morphology of filled composites. Morphology of the rubber composites at different filler loading at 2 phr, 6 phr, 10 phr and 12 phr was investigated by scanning electron microscopy (SEM). Figure 2 shows the filler particles are homogeneously dispersed throughout the rubber matrix with few aggregates at 2 phr filler content in rubber composites (Figure 2a) with increase in filler loading (10 and 12 phr), the aggregation tendency of filler particles increases and it is much dominant for rubber matrix filled with 12 phr (Figure 2d). Figure 2d shows the particle size distribution is in the range of 100 to 150 nm for smaller particles while size of larger filler particles aggregates lies in the range of 300 to 450 nm. Uniform dispersion of filler into rubber matrix is evident in all surface modified filler composites (Figures 2a-2d).

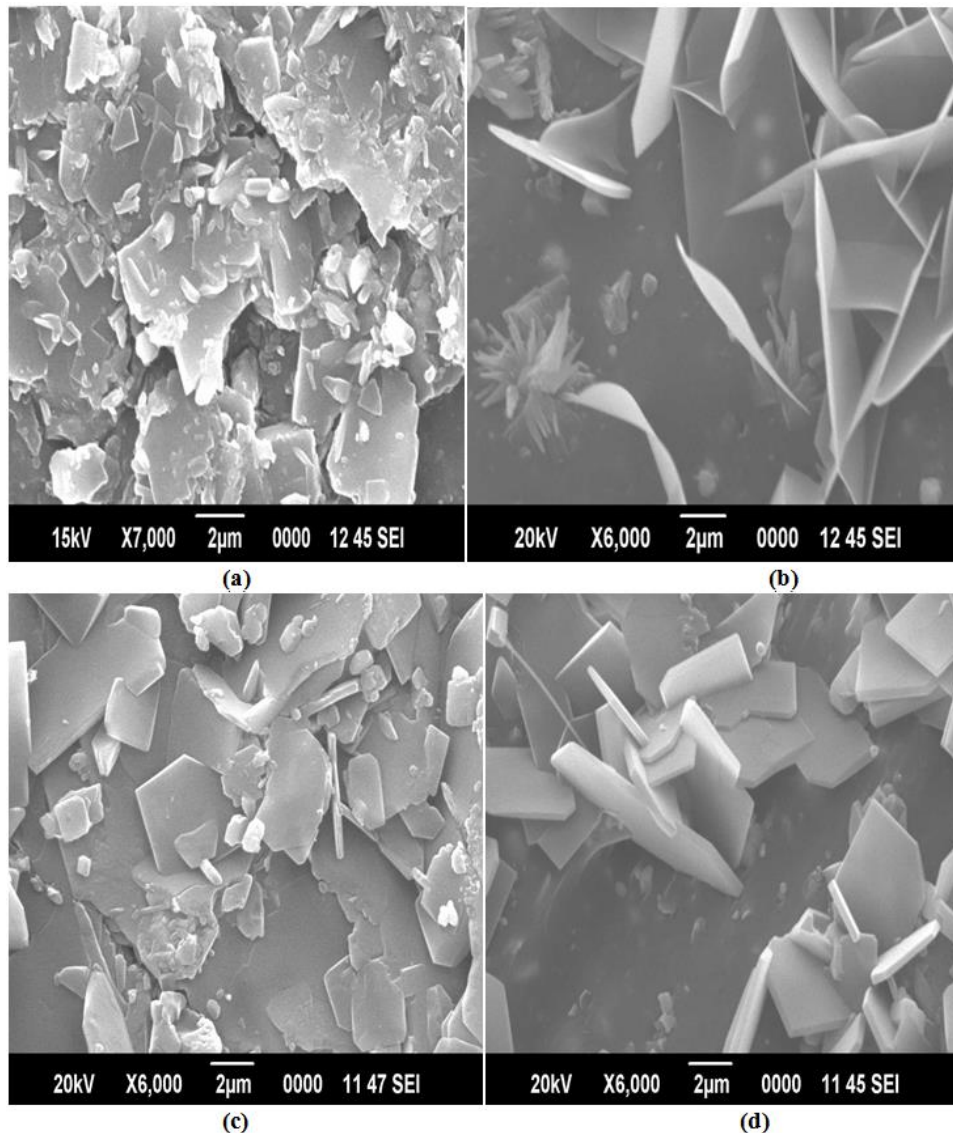


Figure 2: Scanning electron microscopy (SEM) images of SBR-nano composite: (a) 2 phr, filler (b) 6 phr, (c) 10 phr, (d) 12 phr

TEM morphology

TEM measurements are mostly used approaches for morphological analysis. TEM compares the layer dispersion visually and gives a clear picture of the nano particle dispersion. Though the small sample size and requirement of contrast between components of a material makes some disadvantage for TEM, it can provide a confirmation to the dispersion state by providing a visual image, which is much easier to understand. From the TEM analysis it is possible to analyze the effect of nano particles in polymer matrices. It is well known that the nano particles should disperse well in the polymer system. Several measurements can give a general insight into the nano scale dispersion and properties.

In Figures 3a and 3b, the two images given represent pure SBR-nano antimony oxide nano composites. It can be directly observed from the image that a better dispersion and distribution is obtained when the samples are mixed with emulsion method. This shows the delamination of nano antimony oxide or the diffusion of elastomer chains in-between the nano antimony oxide particles. The interlayer spacing created by the solvent molecules during the emulsion mixing, makes it possible for the elastomer chains to diffuse between the nano antimony oxide layers easily. Also, the migration of nano antimony oxide seems to affect the affinity between rubber and the nano antimony oxide, as other factors like viscosity and agglomeration could be less determining factors. The well dispersed filler can interact with the polymer much more in emulsion mixing. The images of SBR-nano antimony oxide nano composites clearly show the better dispersion of nano antimony oxide in the SBR system. The nano antimony oxide is dispersed well, and more number of nano antimony oxide could be observed near the interface. A well dispersed distribution of nano antimony oxide is observed. There is also a better alignment of the nano antimony oxide layers, and more number of intercalated nano antimony oxide layers could be observed near the interface.

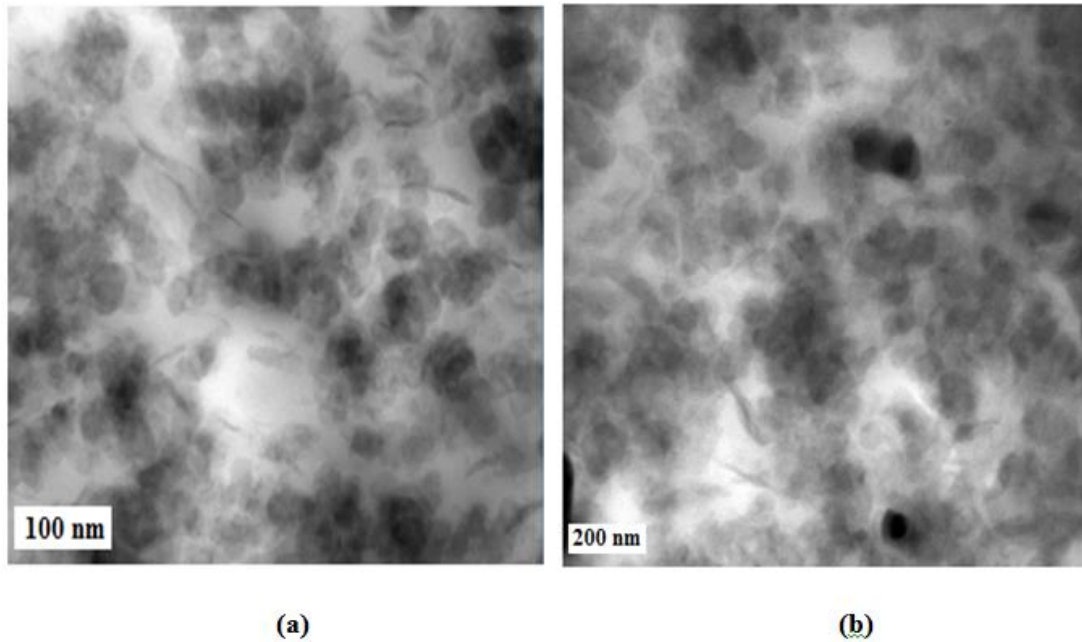


Figure 3: TEM morphology of SBR –nano antimony oxide composites

Mechanical testing

Tensile strength

Addition of nano antimony oxide (Figure 4) shows an increase of the tensile strength. As the concentration increases, tensile strength increases. Such behavior can be explained that nano particles will fill the spaces between rubber chains, thus giving a rigid structure with better tensile strength (14.2 Mpa). The value of tensile strength is shown in Table 3. Intercalation of rubber chains into the layers resulted in an increase in tensile strength. The enhancement in properties occurs because of the higher polymer filler interactions than filler-filler interactions. The functional groups are incorporated into the polymer; the stress is much more efficiently transferred from the polymer matrix to the inorganic filler, resulting in a higher increase in tensile properties. The driving force for intercalation originates from the strong hydrogen bonding. An increment of tensile strength is observed for SBR rubber and nano antimony oxide.

Table 3: Mechanical properties of SBR unfilled and filled nano antimony oxide composites

Compounds	1	2	3	4	5
$\sigma_{100\%}$ (MPa)	2.3	2.4	2.5	2.8	3.2
$\sigma_{200\%}$ (MPa)	2.5	2.6	2.9	3.2	3.5
$\sigma_{300\%}$ (MPa)	2.8	2.9	3.2	3.5	3.8
Tensile strength, Mpa	12.1	12.2	13	13.8	14.2
Elongation at break, %	460	520	540	550	550
Tear resistance, Mpa	4.7	5.2	5.9	6.2	6.4
Abrasion resistance, %	20	20	13	12	10
Cross-link density $n \times 10^{-4}$	2.63	3.95	4.85	5.8	6.11

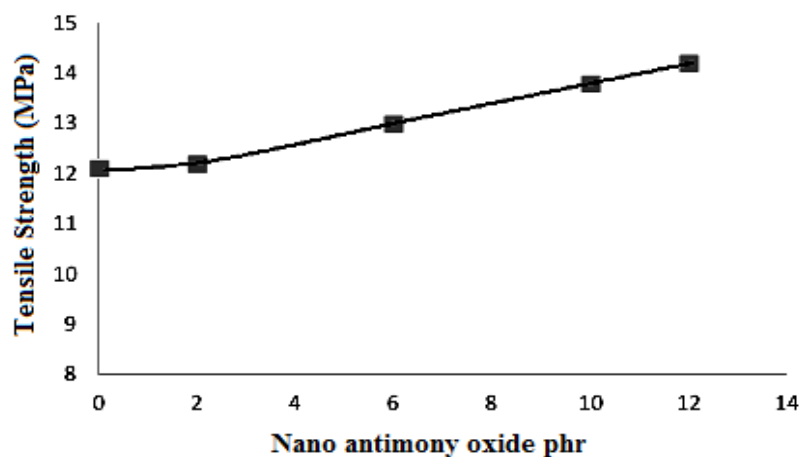


Figure 4: Shows the effect of nano antimony oxide on tensile strength

Elongation property

The elongation property increases with the addition of nano antimony oxide as shown in Figure 5. This is due to the diffusion of very fine nano antimony oxide particles through the rubber chains and supports the rubber chains so enhanced stretching which reflect on elongation. The value of maximum elongation at break is shown in Table 3. Figure 5 is the elongation at break (%) curves of nano composites containing varying percentage of nano antimony oxide. The elongation at break of all systems increases with increase in weight percentage of filler. The increase at higher loading is due to the enhancement in rigidity of the material and was possibly caused by the reduction in tensile crystallization. All the system shows the same trend. For most of the applications requiring a large initial reinforcement, the ultimate strain is not very crucial.

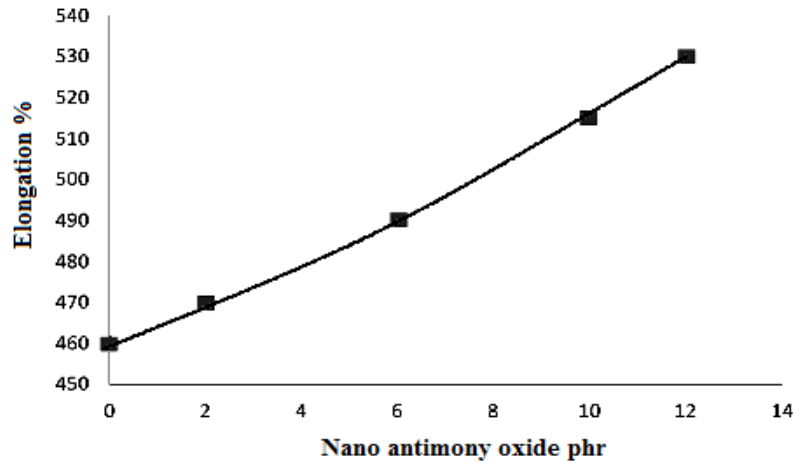


Figure 5: Shows the effect of nano antimony oxide on elongation property

Tear resistance property

This property related to the tensile property so that tear resistance increases with increasing quantities of the nano antimony oxide as (Figure 6) it reaches to a maximum value of 6.4 Mpa at 12 pphr of nano antimony oxide for the same reason as previously mentioned in the case of tensile property that the particles will fill the spaces between rubber chains and increase the mechanical bond between them this lead to better tear resistance. Figure 6 is the tear strength curves of the system as a function of weight percentage of nano antimony oxide content. SBR rubber filled nano antimony oxide shows an increment in tear strength, indicating the resistance offered in the SBR rubber in order to enhance the crack propagation and the super reinforcement of nano antimony oxide. Above all, the finely dispersed rubber layers divert the tear path, which in turn imparts high tear strength to nano composites.

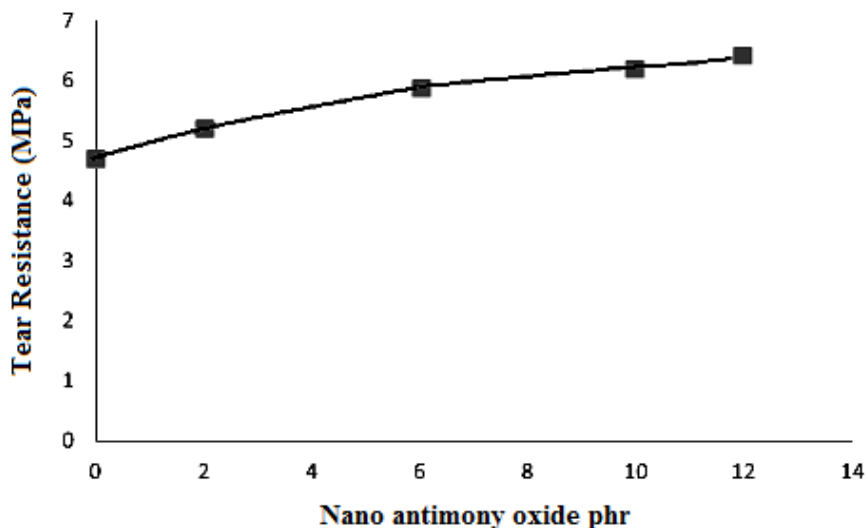


Figure 6: Shows the effect of nano antimony oxide on tear resistance property

Abrasion resistance property

Figure 7 shows that the addition of nano antimony oxide in SBR matrix e.g. 2 pphr, the weight loss of rubber is constant and for 10 pphr, the weight loss of rubber is again decreases until it reaches 10% because nano particles will be restrict weight loss. As the hardness increases abrasion loss, which is a measure of reinforcement, should decrease and this is reflected in Figure 7. The increased crosslink density which results in increased hardness and modulus ultimately gives rise to the enhancement of abrasion resistance. It can be observed that decrease abrasion loss is observed. This improved abrasion resistance in the SBR-nano antimony oxide filled composites is also due to the improved rubber-filler interaction. The intercalation and exfoliation of the modified silicate increased the surface area of the filler, leading to more interaction between the filler and the matrix.

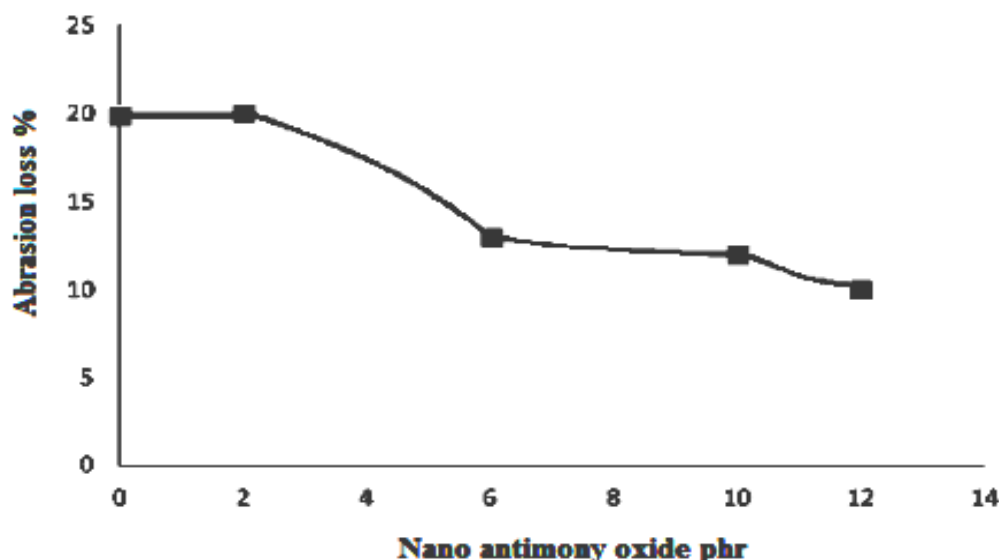


Figure 7: Shows the effect of nano antimony oxide on abrasion resistance property

CONCLUSION

Addition of nano- antimony oxide in SBR rubber is improved the FTIR and mechanical properties. This is due to the fact that nano antimony oxide acts as a filler to fill the spaces in the SBR composites so that improved the properties of rubber nano composites. Morphology of rubber-nano composite shows the filler particles are homogenously dispersed throughout the rubber matrix. TEM analysis of rubber-nano composites shows the diffusion of elastomer chains in-between the nano antimony oxide particles. The interlayer spacing created by the solvent molecules during the emulsion mixing, makes it possible for the elastomer chains to diffuse between the nano antimony oxide layers easily. Emulsion polymerization method causes to much more improvement in the properties. Nano antimony oxide gives the better tensile strength, tear resistance and abrasion loss. The elongation property increases with the increase of nano antimony oxide concentration, this is due to the diffusion of nano antimony oxide through the rubber chains and supports the rubber bond so enhanced stretching.

ACKNOWLEDGEMENT

The authors are thankful to Sophisticated Analytical Instruments Facility, SAIF, Cochin for elemental analysis results. Authors are also thankful to Mumbai University, Mumbai for carrying out mechanical testing of the rubber-nano composites.

REFERENCES

- [1] G. Heinrich, M. Kluppel, T.A. Vilgis, *Current Opinion in Solid State & Materials Science.*, **2002**, 6(3), 195-203.
- [2] W.D. Harkins, *J. Am. Chem. Soc.*, **1947**, 69, 1428-1444.
- [3] W.V. Smith, R.H. Ewart, Kinetics of emulsion polymerization, *J. Chem. Phys.*, **1948**, 16, 592-599.
- [4] C.S. Chern, Emulsion polymerization mechanisms and kinetics, *Prog. Polym. Sci.*, **2006**, 31, 443-486.
- [5] S.C. Thickett, R.G. Gilbert, *Polymer.*, **2007**, 48, 6965-6991.
- [6] J.E. Mark, B. Erman, F.R. Eirich, *Science and Technology of Rubber*, Academic Press: San Diego, **1994**.
- [7] D.J. Kohls, G. Beaucage, *Current Opinion in Solid State & Materials Science.*, **2002**, 6(3), 183-194.
- [8] A. Nakatani, W. Chen, R. Schmidt, G. Gordon, C. Han, *Polymer.*, **2001**, 42, 3713-3722.
- [9] N. Jouault, F. Dalmas, S. Said, E. Di Cola, R. Schweins, J. Jestin, F. Boue, *Macromolecules.*, **2010**, 43(23), 9881.
- [10] K. Nusser, S. Neueder, G.J. Schneider, M. Meyer, W. Pyckhout-Hintzen, L. Willner, A. Radulescu, D. Richter, *Macromolecules.*, **2010**, 43(23), 9837-9847.
- [11] A.C. Genix, M. Tatou, A. Imaz, J. Forcada, I. Grillo, J. Oberdisse, *Macromolecules.*, **2012**, 45(3), 1663-1675.
- [12] G. Tsagaropoulos, A. Eisenberg, *Macromolecules.*, **1995**, 28(1), 396-398.
- [13] J. Berriot, H. Montes, F. Lequeux, D. Long, P. Sotta, *Macromolecules.*, **2002**, 35 (26), 9756-9762.
- [14] G.J. Papakonstantopoulos, M. Doxastakis, P.F. Nealey, J.L. Barrat, J.J. de Pablo, *Physical Review E.*, **2007**, 75(3).
- [15] J. Frohlich, W. Niedermeier, H.D. Luginsland, *Composites Part a-Applied Science and Manufacturing.*, **2005**, 36(4), 449-460.
- [16] C.G. Robertson, M. Rackaitis, *Macromolecules.*, **2011**, 44(5), 1177-1181.
- [17] C. Chevigny, N. Jouault, F. Dalmas, F. Boue, J. Jestin, *Journal of Polymer Science Part B-Polymer Physics.*, **2011**, 49(11), 781-791.
- [18] J. Gao, A. Penlidis, *Prog. Polym. Sci.*, **2002**, 27, 403-535.
- [19] E. Saldivar, P. Dafiniotis, W.H. Ray, *J. Macromol. Sci. R. M. C.*, **1998**, 38, 207-325.
- [20] R.V. Mankar, W.B. Gurnule, *Res. J. Pharm., Bio. Chemical Sci.*, **2018**, 9(5) 791-799.
- [21] L. Conzatti, G. Costa, M. Castellano, A. Turturro, F.M. Negroni, J.F. Gerard, *Macromolecular Materials and Engineering.*, **2008**, 293(3), 178-187.
- [22] J. Kanetakis, F.Y.C. Wong, A.E. Hamielec, J.F. MacGregor, Steady-state modeling of a latex reactor train for the production of styrene-butadiene rubber, *Chem. Eng. Commun.*, **1985**, 35, 123-140.
- [23] J. Ramier, C. Gauthier, L. Chazeau, L. Stelandre, L. Guy, *J. Polymer Sci. Part B-Polymer Phys.*, **2007**, 45(3), 286-298.
- [24] L.H. Sperling, *Introduction to physical polymer science*, Wiley, **2005**.